Supplementary Materials

Kub5-Hera*RPRD1B* deficiency promotes "BRCAness" and vulnerability to PARP inhibition in BRCA-proficient Breast Cancers

Edward A. Motea[1§*], Farjana J. Fattah[1], Ling Xiao[1], Luc Girard[2], Amy Rommel[3], Julio C. Morales[4], Praveen L. Patidar[5], Yunyun Zhou[6#], Andrew C. Porter[7], Yang Xie[6], John D. Minna[2], David A. Boothman[1§*]

[1]Departments of Pharmacology and Radiation Oncology, Simmons Comprehensive Cancer Center, University of Texas Southwestern Medical Center, Dallas, TX, USA
[2]Hamon Center for Therapeutic Oncology Research, University of Texas Southwestern Medical Center, Dallas, TX, USA
[3]Laboratory of Genetics, The Salk Institute for Biological Studies, La Jolla, CA, USA
[4]Department of Neurosurgery, University of Oklahoma Health Science Center, Oklahoma City, OK, USA
[5]Department of Chemistry, New Mexico Institute of Mining and Technology, Socorro, NM, USA
[6]Department of Clinical Science, University of Texas Southwestern Medical Center, Dallas, Texas, USA
[7]Center for Hematology, Imperial College, London, UK

Present Address: [#]Department of Data Science, John D. Bower School of Population Health, University of Mississippi Medical Center, Jackson, MS, USA; [§]Department of Biochemistry and Molecular Biology, Melvin and Bren Simon Cancer Center, Indiana University School of Medicine, Indianapolis, IN, USA

[*]Correspondence: *eamotea@iu.edu*
or
dboothm@iu.edu

Figure S1

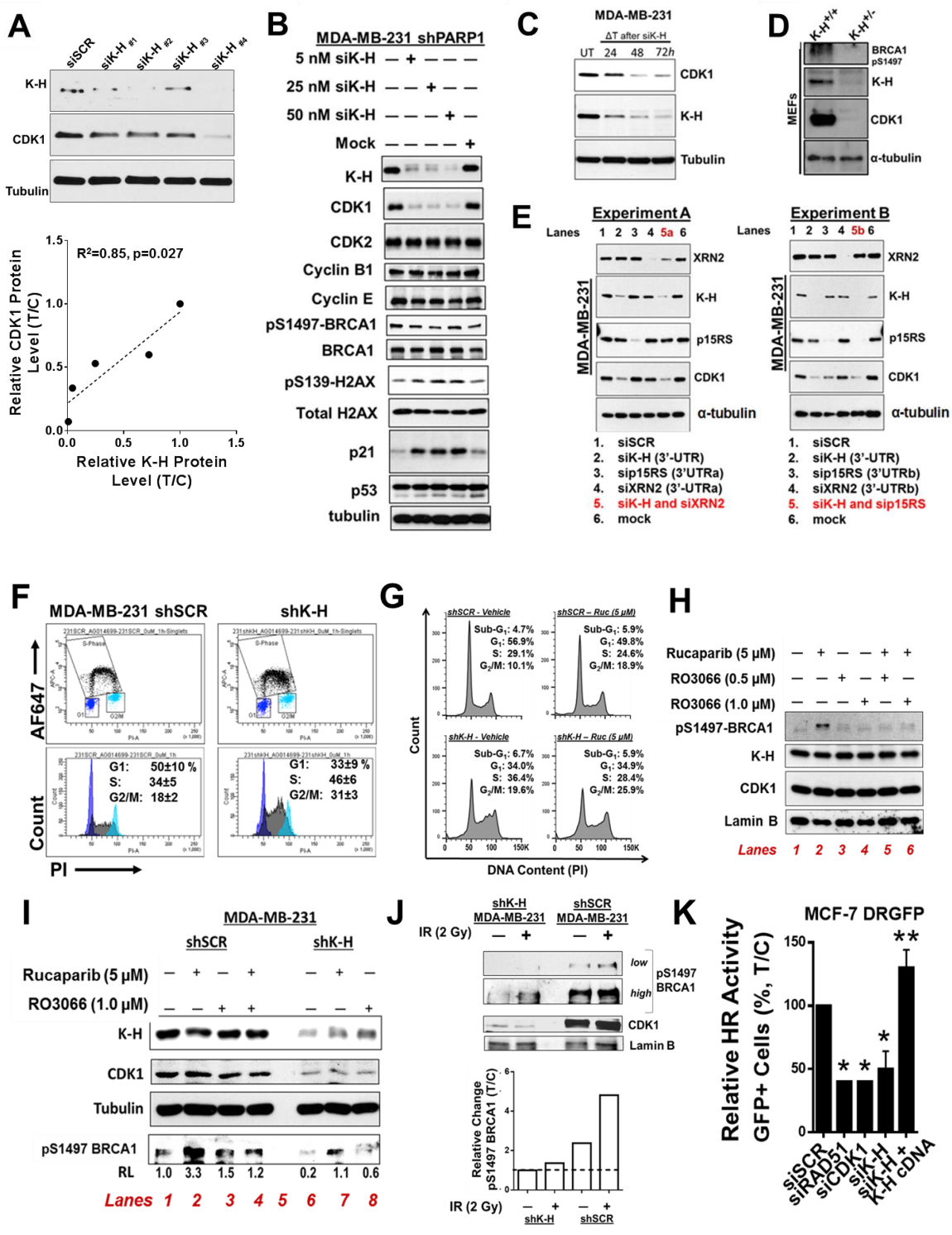
A
siSCR
siK-H #1
siK-H #2
siK-H #3
siK-H #4
K-H
CDK1
Tubulin
R²=0.85, p=0.027
Relative CDK1 Protein Level (T/C)
Relative K-H Protein Level (T/C)
B
MDA-MB-231 shPARP1
5 nM siK-H
25 nM siK-H
50 nM siK-H
Mock
K-H
CDK1
CDK2
Cyclin B1
Cyclin E
pS1497-BRCA1
BRCA1
pS139-H2AX
Total H2AX
p21
p53
tubulin
C
MDA-MB-231
ΔT after siK-H
UT 24 48 72h
CDK1
K-H
Tubulin
D
K-H+/+
K-H+/-
MEFs
BRCA1 pS1497
K-H
CDK1
α-tubulin
E
Experiment A
Lanes 1 2 3 4 5a 6
MDA-MB-231
XRN2
K-H
p15RS
CDK1
α-tubulin
1. siSCR
2. siK-H (3'-UTR)
3. sip15RS (3'UTRa)
4. siXRN2 (3'-UTRa)
5. siK-H and siXRN2
6. mock
Experiment B
Lanes 1 2 3 4 5b 6
MDA-MB-231
XRN2
K-H
p15RS
CDK1
α-tubulin
1. siSCR
2. siK-H (3'-UTR)
3. sip15RS (3'UTRb)
4. siXRN2 (3'-UTRb)
5. siK-H and sip15RS
6. mock
F
MDA-MB-231 shSCR
shK-H
AF647
PI
G1: 50±10 %
S: 34±5
G2/M: 18±2
G1: 33±9 %
S: 46±6
G2/M: 31±3
G
shSCR - Vehicle
shSCR – Ruc (5 μM)
shK-H - Vehicle
shK-H – Ruc (5 μM)
Count
DNA Content (PI)
H
Rucaparib (5 μM)
RO3066 (0.5 μM)
RO3066 (1.0 μM)
pS1497-BRCA1
K-H
CDK1
Lamin B
Lanes 1 2 3 4 5 6
I
MDA-MB-231
shSCR
shK-H
Rucaparib (5 μM)
RO3066 (1.0 μM)
K-H
CDK1
Tubulin
pS1497 BRCA1
RL 1.0 3.3 1.5 1.2 0.2 1.1 0.6
Lanes 1 2 3 4 5 6 7 8
J
shK-H MDA-MB-231
shSCR MDA-MB-231
IR (2 Gy)
low
high
pS1497 BRCA1
CDK1
Lamin B
Relative Change pS1497 BRCA1 (T/C)
IR (2 Gy)
shK-H
shSCR
K
MCF-7 DRGFP
Relative HR Activity GFP+ Cells (%, T/C)
siSCR
siRAD51
siCDK1
siK-H
siK-H + K-H cDNA

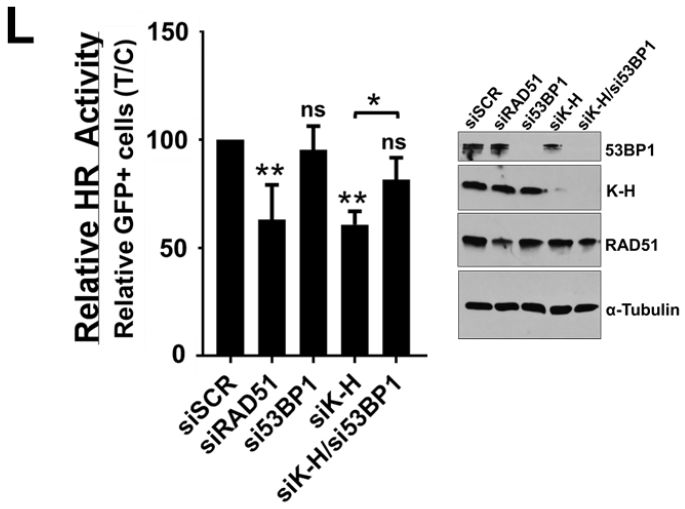

Fig. S1: Loss of K-H compromises CDK1 expression/activity and reduces HR-mediated DSB repair.

(**A**) Western blot analysis of K-H, CDK1 protein levels in 231 cells treated with siSCR or four different siRNA to knockdown K-H (15 nM, 48 h). siK-$H_{\#4}$ was used throughout the paper. Please see Table S4 for siRNA sequences.

(**B**) 231 shPARP1 cells transiently transfected with indicated concentrations of siK-H for 48 h. Total cellular proteins from each treatment were subjected to Western blot analysis using indicated antibodies.

(**C**) Western blot analysis of CDK1 protein levels in 231 shSCR cells treated with siK-H (15 nM) and harvested at various times (24, 48, 72 h).

(**D**) Western blot analysis of CDK1 and phospho-BRCA1 (pS1497) protein levels in K-H wild-type (*K-H*$^{+/+}$) versus K-H het (*K-H*$^{+/-}$) mouse embryonic fibroblasts (MEFs) cells.

(**E**) Western blot analysis of CDK1 protein levels in 231 cells treated with siRNA to nonspecific gene control (siSCR) or specific pre-mRNA processing genes as indicated (15 nM, 48 h). Specific siRNA oligonucleotide sequence used in this study are listed in **Table S3**.

(**F**) Asynchronous 231 shSCR versus shK-H cells pulsed with 5-ethynyl-2'-deoxy-Uridine (EdU, 10 μM, 1 h) at log phase. See Supplemental Procedure for more details.

(**G**) Cell cycle analyses of asynchronous 231 shSCR versus shK-H cells treated with 0.1% DMSO or Rucaparib (5 µM) for 24 h.

(**H**) 231 cells treated with PARP1i Rucaparib (5 µM, 24 h), CDK1 inhibitor RO3066 (0.5 and 1 µM, 24 h) or combination [Rucaparib+RO3066]. Cells were harvested after 24 h treatment. The immunoblot shows no further reduction of CDK1 after Rucaparib and/or RO3066 treatment. BRCA1 was activated (pS1497-BRCA1) after Rucaparib treatment alone (lane 2) but not in combination with CDK1 inhibitor, RO3066 (lanes 5 and 6). Compromising CDK1 activity has been shown to inhibit BRCA1 phosphorylation at S1497 site, and impairs HR-mediated DSB repair [1, 2].

(**I**) Comparison of 231 cells (shSCR versus shK-H) treated with Rucaparib (5 µM, 24 h), CDK1 inhibitor RO3066 (1 µM, 24 h) or combination [Rucaparib+RO3066]. Cells were harvested after 24 h treatment. The blot shows reduction of CDK1 protein level in shK-H (lanes 6-8), but not in shSCR cells (lanes 1-4). No further reduction of CDK1 protein level was seen after Rucaparib and/or RO3066 treatments. Endogenous pS1497-BRCA1 was higher in vehicle-treated shSCR (lane 1) compared to shK-H (lane 6). Treatment with Rucaparib engaged more pS1497-BRCA1 activation in shSCR cells (lane 2), but was inhibited in combination with CDK1 inhibitor treatment (lane 4) (results similar to (G)). 231 shSCR cells treated with both Rucaparib and RO3066 CDK1 inhibitor exhibited comparable pS1497-BRCA1 activation as 231 shK-H cells treated with Rucaparib only where CDK1 expression/activity is already compromised (compare lane 4 vs. 7).

(**J**) 231 cells treated with ionizing radiation (IR, 2 Gy) and harvested after 1h. *Top*, The blot shows reduction of CDK1 in shK-H compared to shSCR, but no further reduction of CDK1 protein level was observed after IR treatment. *Bottom*, Endogenous phospho-S1497 BRCA1 is higher in shSCR compared to shK-H. After IR treatment, S1497 BRCA1 phosphorylation is impaired in 231 shK-H, but not in shSCR. *High* or *Low* denotes exposure time interval.

(**K**) Homologous recombination assay in MCF-7 cells using DR-GFP reporter system. Columns represent mean percentage of GFP-positive cells normalized to

control (siSCR); error bars represent ± SEM from duplicate experiments, *p<0.05, **p<0.01. See **Table S3** for siRNA sequences. siK-H used was to 3'-UTR.

(**L**) *Right,* Homologous recombination assay in 293DR-GFP cells. Columns represent mean percentage of GFP-positive cells normalized to control (siSCR); error bars represent ± SEM from duplicate experiments, *p<0.05, **p<0.01. *Left,* Western blot confirming knockdown of indicated protein(s).

Figure S2

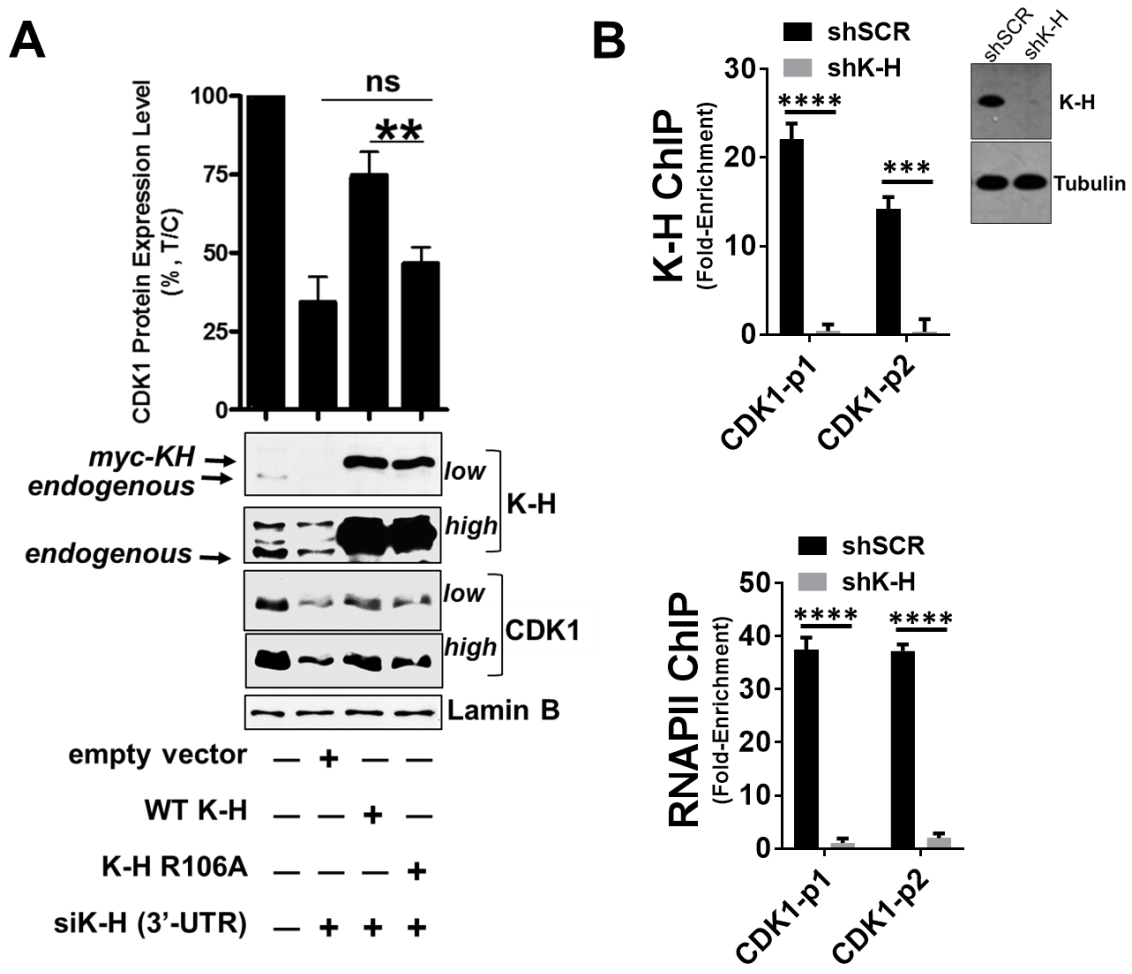

Fig. S2: K-H promotes CDK1 expression by localizing RNAPII. (**A**) Experiments showing rescue of CDK1 protein level after wildtype K-H re-expression in K-H depleted MDA-MB-231 cells (3'-UTR siK-H). K-H (p.R106A) mutant did not show significant rescue of CDK1 protein level. Lamin B was used as loading control for nuclear protein extracts. Columns represent mean CDK1 protein expression level. (**B**) K-H and RNAPII ChIP at the CDK1 promoter region using two different sets of primers (CDK1-p1 and p2) specific to CDK1 promoter. ChIP assay was performed in MDA-MB-231 shSCR and shK-H cells (inset, Western blot protein confirmation). Error bars represent ± s.e.m. from two repeats, **p<0.01, ***p<0.001, ****p<0.0001, ns = not significant.

Figure S3

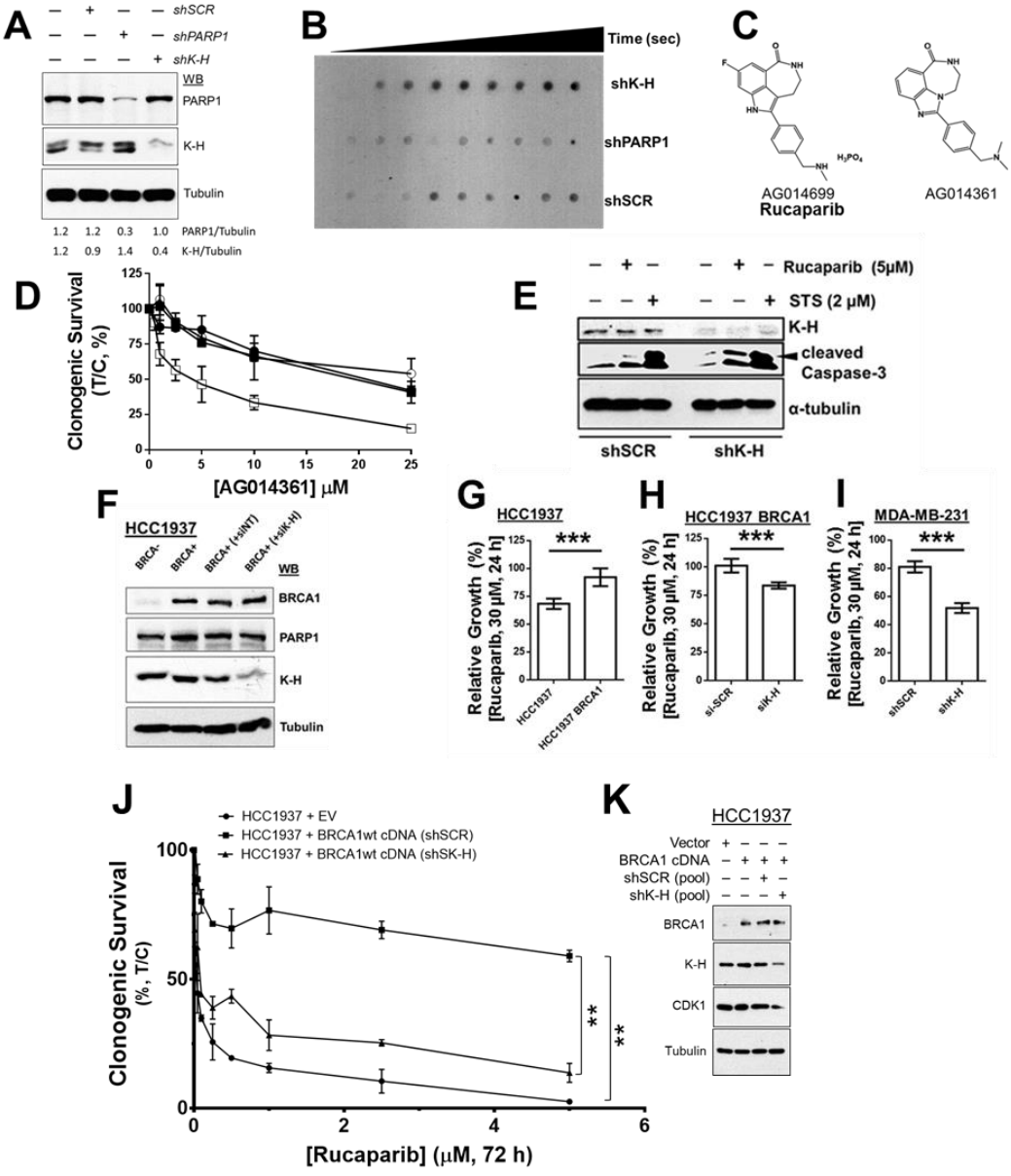

Fig. S3: Pharmacological and genetic ablation of PARP1 activity is synthetic lethal with aberrant K-H reduction in BRCA-proficient breast cancers. (**A**) Western blot analysis of the parental BRCA-proficient 231 TNBC compared with 231 cells engineered to generate stable short hairpin RNA targeting non-specific gene control (shSCR), Kub5-Hera (shK-H) or PARP1 (shPARP1).

(**B**) Representative dot blot of poly(ADP-ribose) to measure PARP activity over time using normalized cell lysates from shSCR, shK-H, or shPARP1 MDA-MB-231 cell lines.

(**C**) Chemical structures of PARP inhibitors used in this study. *Left*, AG014361; *Right*, AG014699 or Rucaparib.

(**D**) Colony formation of specified cell lines treated with varying concentrations (0, 1, 2.5, 5, 10, 25 μM) of PARP inhibitor, AG014361, for 24 h. AG014361 is a less potent analog of the clinically relevant PARP inhibitor, Rucaparib. Survival is expressed as mean percentage of colonies formed relative to vehicle-treated (0.1% DMSO) cells; error bars represent ± SEM from three replicates.

(**E**) Total cellular proteins from indicated 231 cells treated with vehicle (0.1% DMSO), AG014699/Rucaparib (5 μM), or staurosporine (STS, 2 μM) were subjected to Western blot analysis with indicated antibodies.

(**F**) Western blot analysis of HCC1937 cell lines stably transfected with empty vector (lane 1), BRCA1 cDNA (lane 2), BRCA1 cDNA + transient siSCR (lane 3), or BRCA1 cDNA + transient siK-H (lane 4).

Cells in (**E**) were subjected to Rucaparib (30 μM) treatment for 24 h, then allowed to grow in drug-free media until confluent. Since HCC1937 cells do not perform robust colony formation ability, viability was measured using Sulforhodamine B Assay as previously described [3]. Colorimetric intensity values were obtained using a plate reader, and normalized to control (0.1% DMSO).

(**G**) Comparison of growth inhibition after Rucaparib treatment in [HCC1937 + empty vector] versus [HC1937 + BRCA1 cDNA]. Rucaparib treatment is described above. Data are %means ± SEM from three replicates; ***p<0.001.

(**H**) Comparison of growth inhibition after Rucaparib treatment in [HC1937+ BRCA1 cDNA] cells transiently transfected with siSCR versus siK-H (15 nM, 48 h). Rucaparib treatment is described above. Data are %means ± SEM from three independent experiments; ***p<0.001.

(**I**) Comparison of growth inhibition after Rucaparib treatment in MDA-MB-231 cells transiently transfected with siSCR versus siK-H (15 nM, 48 h). Rucaparib

treatment is described above. Data are %means ± SEM from three independent experiments; ***p<0.001.

(**J**) Clonogenic Survival Assay comparing BRCA1-mutant HCC1937+empty vector (EV) with BRCA1-reconsituted HCC1937+BRCA1$_{wt}$ cDNA cell lines stably integrated with shSCR or shK-H. Each cell line was treated with varying doses of Rucaparib (for 72 h, then allowed to form colonies for >2 weeks (HCC1937 doubling time is ~50 h)).

(**K**) Western blot confirmation of cell lines used in J.

Figure S4

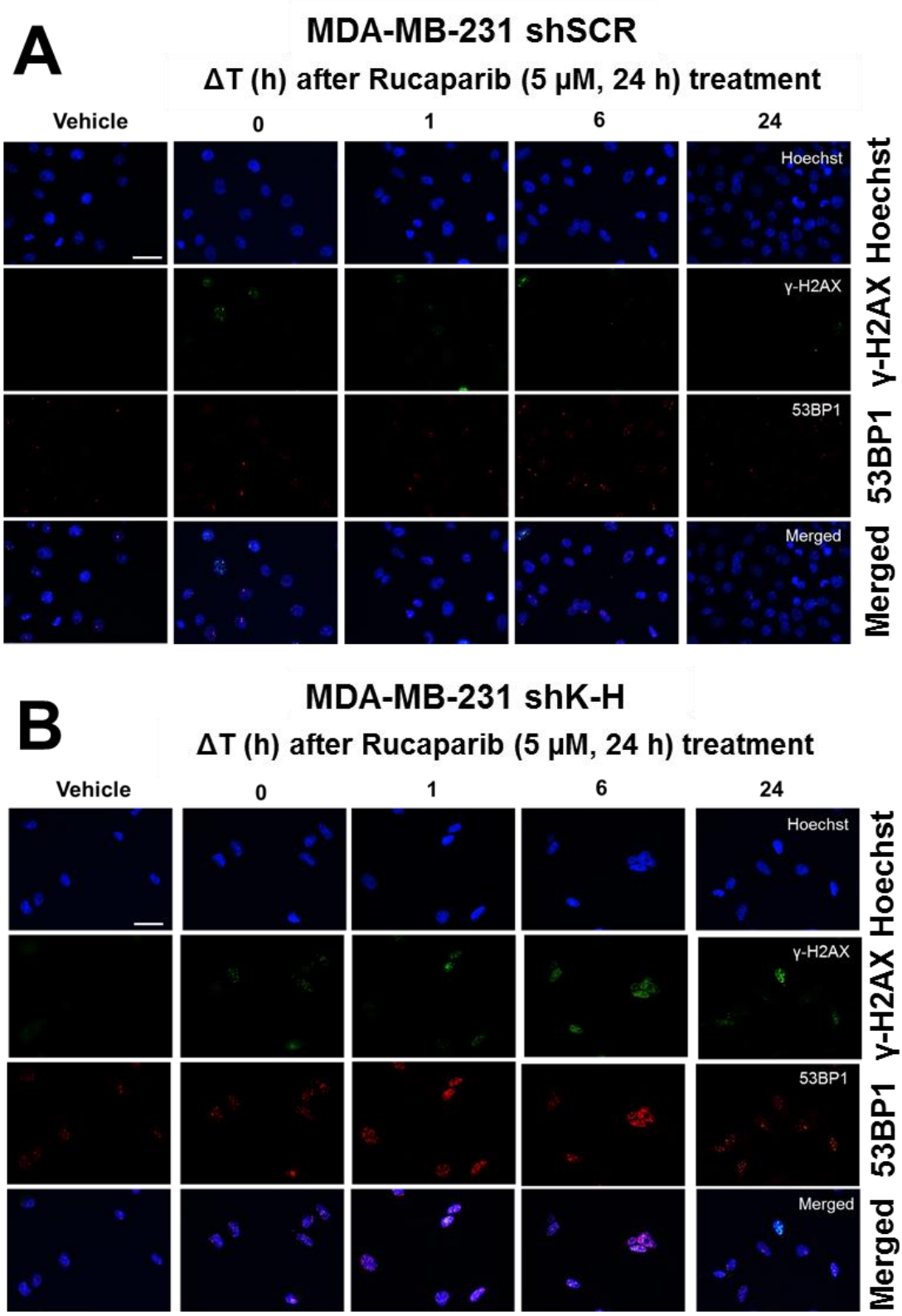
A
MDA-MB-231 shSCR
ΔT (h) after Rucaparib (5 μM, 24 h) treatment
Vehicle
0
1
6
24
Hoechst
γ-H2AX
53BP1
Merged
B
MDA-MB-231 shK-H
ΔT (h) after Rucaparib (5 μM, 24 h) treatment
Vehicle
0
1
6
24
Hoechst
γ-H2AX
53BP1
Merged

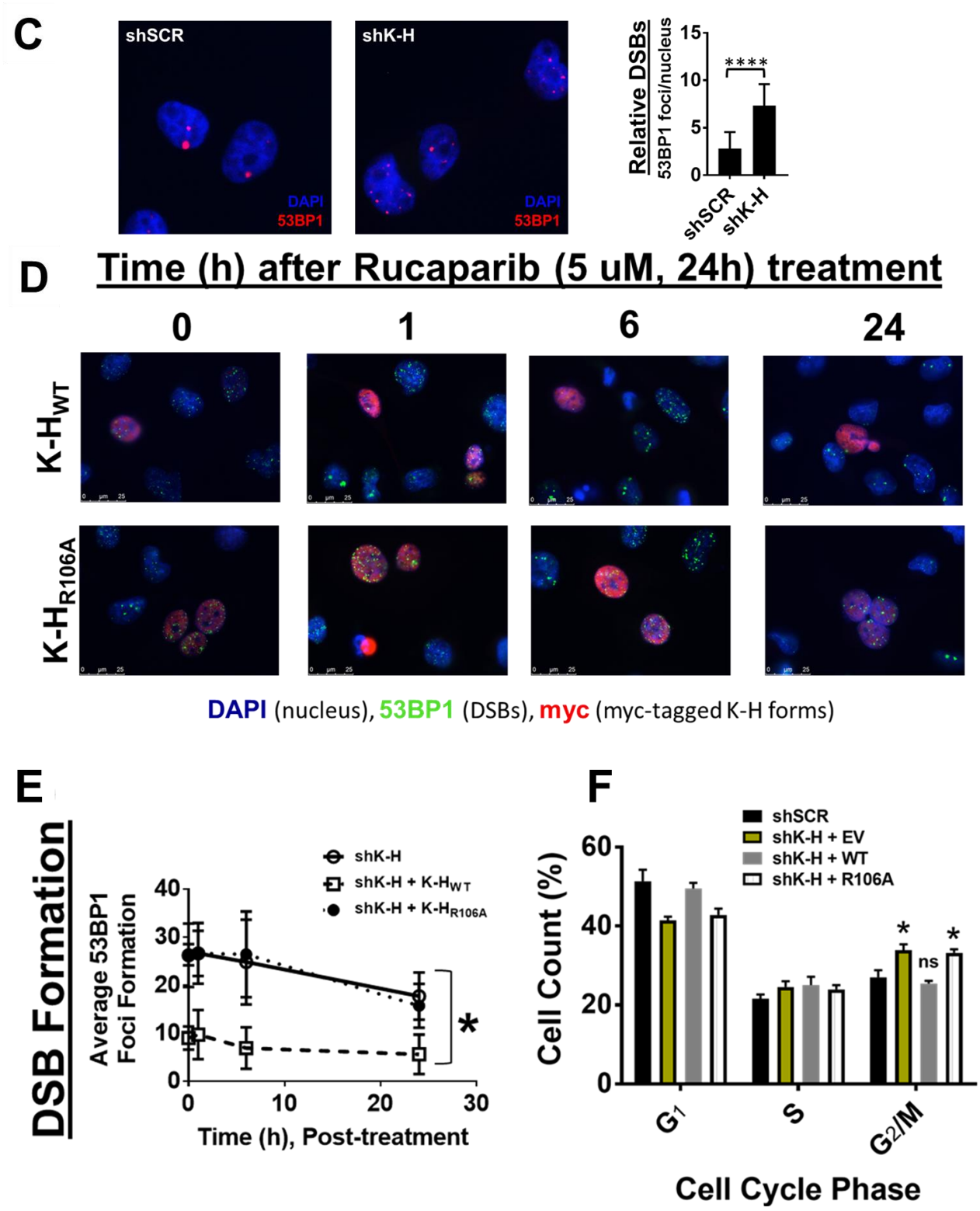

Fig. S4: Representative images for γ-H2AX and 53BP1 foci formation, surrogate DSB markers, over time in (**A**) shSCR or (**B**) shK-H 231 cells after vehicle

(0.01% DMSO) or Rucaparib treatment for 24 h. DAPI stained cell nuclei. Scale bar: 30 µm.

(**C**) Representative images for endogenous 53BP1 foci formation (in red, surrogate DSB markers) in MDA-MB-231 shSCR versus shK-H cells. Quantitation is shown on the left, ****p<0.0001.

(**D**) Representative images for 53BP1 foci formation (in green, surrogate DSB markers) over time in MDA-MB-231 shK-H cells transiently transfected with myc-tagged-K-H wild-type versus R106A mutant cDNA (in red), then treated with vehicle (0.1% DMSO) or Rucaparib (5 µM) for 24 h. DAPI stained cell nuclei. Scale bar: 30 µm.

(**E**) Quantitation of DSB formation over time in (C).

(**F**) Cell cycle profile of asynchronous MDA-MB-231 shSCR compared to shK-H cells re-expressed with empty pCMV vector, K-H wild-type, or K-H R106A mutant cDNA. Data are %means ± SEM from triplicate experiments; *p<0.05; ns=not significant.

Figure S5

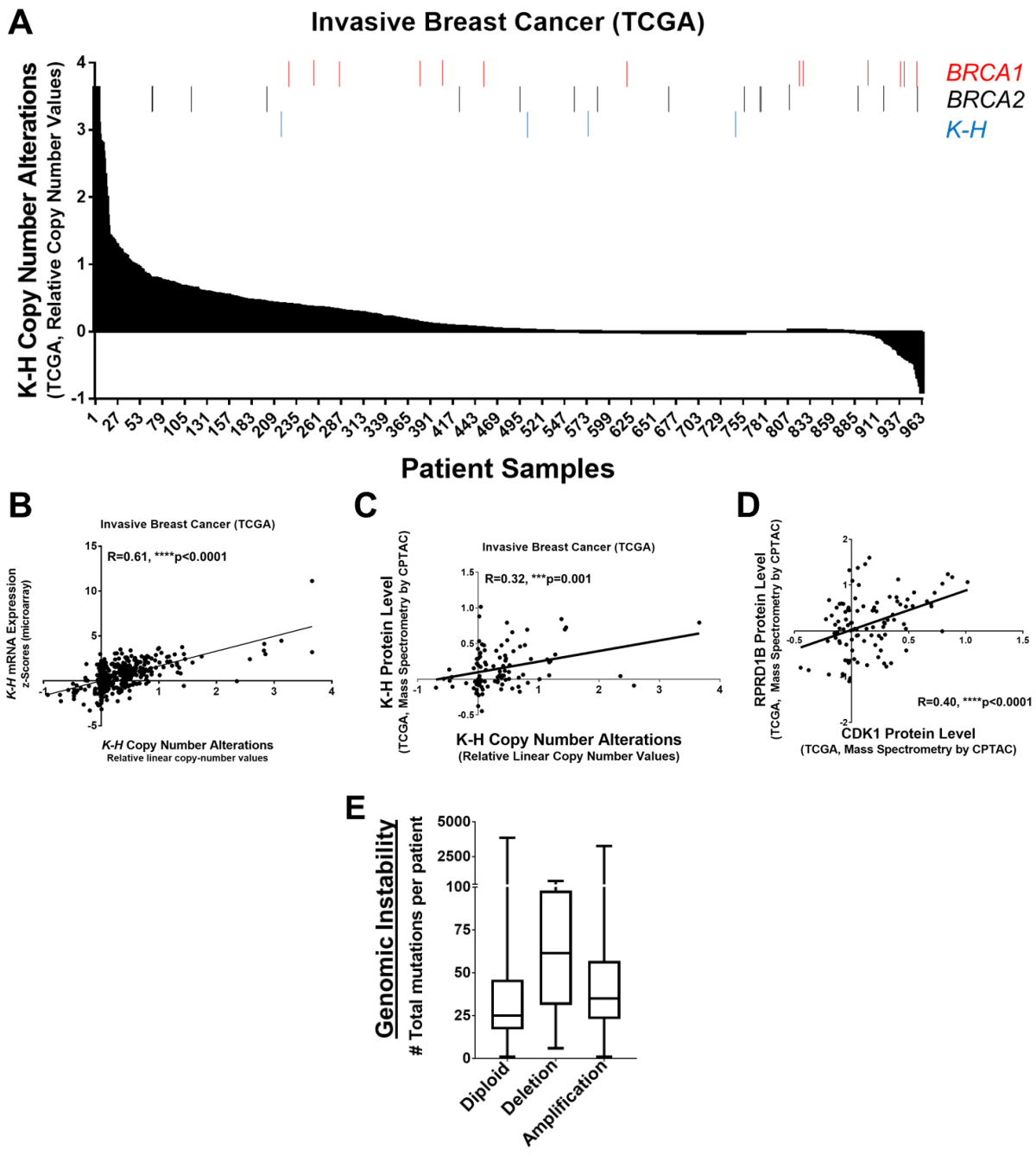

Fig. S5: Distribution of *K-H* Copy Number Alterations (CNA) and mRNA expression in invasive breast cancer patients derived from The Cancer Genome Atlas (TCGA, Provisional)*.

(**A**) Waterfall plot demonstrating the distribution of copy number alterations (relative copy number values) in breast cancer TCGA (tumors with sequencing

and CNA data); (+) represents amplification and (—) represents deletion of *K-H* copy number. Approximately 18% of breast cancer patients show deletion of *k-h* copy number. Tick marks above represent patients with mutations in *BRCA1* (red), *BRCA2* (black), and *K-H* (blue). Note that mutations in BRCA1/2 is not exclusive to patient samples with *K-H* loss.

(**B**) Correlation between *K-H* mRNA expressions versus *K-H* CNA in breast cancer TCGA data.

(**C**) Correlation between *K-H* CNA versus K-H protein level in breast cancer TCGA data. Note that these results closely resemble the data obtained in a panel of breast cancer cell lines used in this study.

(**D**) Correlation between CDK1 Protein level versus K-H protein in invasive breast cancer TCGA data. Protein abundance was obtained through National Cancer Institute's Clinical Proteomic Tumor Analysis Consortium (CPTAC).

(**E**) Whisker plot analyses and comparison of Genomic Instability (represented by the number of gene mutations per patient) in patients (n=963) with Invasive Breast Cancer with *K-H* diploid, *K-H* deletion, and *K-H* amplification (GISTIC Threshold Output).

*The results shown here are based upon data generated through www.cbioportal.org and the TCGA Research network: http://cancergenome.nih.govl

Figure S6

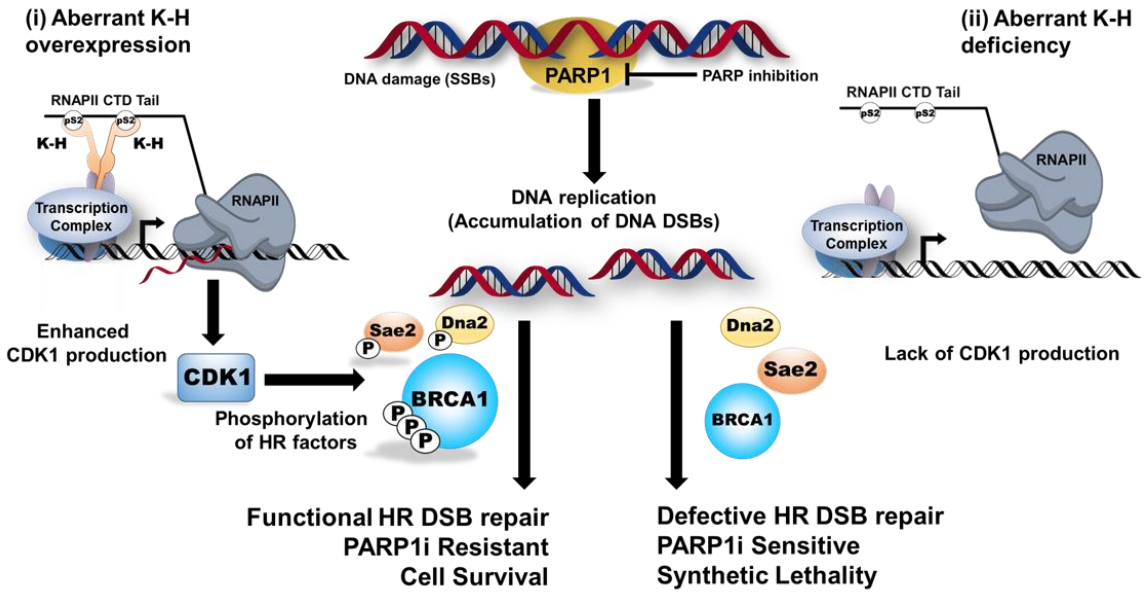

Fig S6: Proposed simplified putative model depicting K-H regulation of CDK1 expression, BRCA1 phosphorylation and HR activity highlighting the potential mechanism of synthetic lethality in K-H-deficient cells combined with PARP1 inhibition.

Table S1: List of altered genes in K-H knocked down MDA-MB-231 cells obtained via Gene Expression Microarrays (p-value ≤0.01, with ≥1.5-fold change in gene expression relative to control (siSCR)). (A) downregulated genes**, (B)** upregulated genes, (**C**) Venn Diagram comparing HR deficient gene signature versus K-H deficient gene alterations, and (**D**) DAVID analysis of overlapping genes in S1C. Please see attached Excel file.

Table S2. Summary of breast cancer cell lines and LC_{50} values obtained in this study.

Breast Cancer Cell Line	ER*	PR*	Her2*	p53*	K-H protein level	AG014699 Mean LC_{50} (SEM) (μM)
HCC1569 (A)	neg	neg	pos	-[M]	0.69	18 (3)
MDA-MB-231 (B)	neg	neg	neg	++[M]	0.46	20 (5)
MCF-7 (L)	pos	pos	neg	+/-[WT]	0.20	11 (2)
HCC202 (L)	neg	neg	pos	-	0.18	6.7 (1)
HTB24 (B)	neg	neg	neg	-[M]	0.14	1.5 (0.1)
HTB122 (B)	neg	neg	neg	++[M]	0.09	3.9 (1.1)
HCC1937[€] (A)	neg	neg	neg	[-]	0.45	ND[‡]
MDA-MB-231 shSCR (B)	neg	neg	neg	++[M]	0.51	18 (5)
MDA-MB-231 shPARP1 (B)	neg	neg	neg	++[M]	0.56	17 (3)
MDA-MB-231 shK-H (B)	neg	neg	neg	++[M]	0.15	0.7 (0.1)

Abbreviations: A = Basal A subtype; B = Basal B subtype; L = Luminal subtype; (—) = protein not expressed; (+) = protein expressed; M = mutant form; WT = wild type form

*****Determined from [4]

AG014699 is also known as Rucaparib. Mean LC_{50} values were obtained from long term colony forming assays. (SEM) denotes standard error of mean from three replicates.

[€]BRCA-mutant breast cancer cell line. [‡]ND means not determined due to inability to perform robustly in a clonogenic assay.

Table S3: Summary of antibodies used in this study.

PRIMARY ANTIBODY	SOURCE	Cat#	Dilution (WB, *IF*, IP)
RPRD1B (K-H)	Sigma	SAB2701444	1:1000, **20 μg (ChIP)**
PARP1	Sta. Cruz	F-2, sc-8007	1:1000
CDK1 (CDC2)	Sta. Cruz	C-19, sc-954	1:1000
pS1497-BRCA1	Sta. Cruz	Sc-12889-R	1:500

CDK2	Sta. Cruz	M2, sc-163	1:500
BRCA1	CalBioChem	OP92	1:500
pS139-H2AX	Thermo Scientific	MA1-2022	1:1000, *1:500*
53BP1	Sta. Cruz	H300, sc-22760	*1:500*
H2AX	Bethyl Laboratories	A300-082A	1:1000
Cyclin E	Sta. Cruz	HE12, sc-247	1:500
Cyclin B1	Sta. Cruz	H-20, sc-594	1:500
Cyclin D1	Sta. Cruz	H-295, sc-753	1:500
p21	Sta. Cruz	F-5, sc-6246	1:500
p53	Sta. Cruz	DO-1, sc-126	1:1000
cleaved Caspase-3	Cell Signaling	9664	1:500
poly(ADP)-ribose (PAR)	Trevigen	4335-mc-100	1:1000
c-myc	Sigma	9E10	1:1000, **2 µg (IP)**
RNA Polymerase II	Bethyl Lab Sta. Cruz	A300653A N-20, sc-899	1:500 **2 µg (ChIP)**
α-tubulin	Sigma	T9026	1:25,000
Lamin B	Sta. Cruz	G1, sc-373918	1:500
p15RS	Sta. Cruz (m) Sta. Cruz (r)	FF-8, sc-81849 L-16, sc-85090	1:1000 1:1000
XRN2	Abcam	72181	1:500
Rad51	Sta. Cruz	H-92, sc-8349	1:1000
SECONDARY ANTIBODY			
Control mouse IgG	Sta. Cruz	sc-2025	**2 µg (IP)**
Control rabbit IgG	Sta. Cruz	sc-2027	**2 µg (ChIP)**
Goat anti-mouse HRP	Sta. Cruz	sc-2031	1:5000-50,000
Goat anti-rabbit HRP	Sta. Cruz	sc-2030	1:2000-5000
Goat anti-mouse Alexa Fluor 488	Life Technologies	A11001	*1:1000*
Donkey anti-rabbit Alexa Fluor 594	Life Technologies	A21207	*1:1000*

Table S4: Summary of siRNA sequences used in this study

siRNA TARGET	**Custom siRNA sequence or Cat. #**	**Source**
siSCR	5′-GACCGUUAGGUACAGAAGAUU-3′	**Dharmacon**
siK-H$_{\#1}$ (3'-UTR)	Sigma-generated sequence	**Sigma**
siK-H$_{\#2}$ (3'-UTR)	Sigma-generated sequence	**Sigma**
siK-H$_{\#3}$ (3'-UTR)	Sigma-generated sequence	**Sigma**
siK-H$_{\#4}$ (3'-UTR)	5'-GGCUGAAACCCAAACUAUAUU-3'	**Dharmacon**

siK-H (pool)	ON-TARGET PLUS (#L-013787-01-0005)	**Dharmacon**
sip15RS (3'UTRa)	5'-GCCCAUGGGCUAUCAACUU[dT][dT]-3'	**Sigma**
sip15RS (3'UTRb)	5'-GUUAAGCAGUGCCACACUA[dT][dT]-3'	**Sigma**
siXRN2 (3'-UTRa)	5'-GGAUCUGAAUUUAUUAUUG[dT][dT]-3'	**Sigma**
siXRN2 (3'-UTRb)	5'-GGAAUAGGAGUACUGGUUU[dT][dT]-3'	**Sigma**
siPARP1 (pool)	ON-TARGET PLUS (#L-006656-03-0005)	**Dharmacon**
siRAD51 (ORF)	SASI_Hs02_00553645	**Sigma**
siCDK1 (ORF)	SASI_Hs01_00044049 Seq. Start 865	**Sigma**

Table S5: Summary of shRNA sequences used in this study

MISSION pLKO.1puro shK-H (coding region)	5'CCGGGCAAGATGTTTCTCTATTGGACTCGAGTCCAATAGAGAAACATCTTGCTTTTTTG-3'	**Sigma**
MISSION pLKO.1puro shSCR	5'-CCGGGCGCGATAGCGCTAATAATTTCTCGAGAAATTATTAGCGCTATCGCGCTTTTT-3'	**Sigma**

Table S6: Chromatin Immunoprecipitation (ChIP) primers

TARGET PROMOTER	**Primer Sequence**	**Source**
ACTIN (f)	5'-CTCAATCTCGCTCTCGCTCT-3'	**Sigma**
ACTIN (r)	5'-CTCGAGCCATAAAAGGCAAC-3'	**Sigma**
CDK1 primer1 (f)	5'-CCTCTTTCTTTCGCGCTCTA-3'	**Sigma**
CDK1 primer 1 (r)	5'-GGACCCCGTTCCTCAATACT-3'	**Sigma**
CDK1 primer 2 (f)	5'-TTTTTCTCTAGCCGCCCTTT-3'	**Sigma**
CDK1 primer 2 (r)	5'-CTCTCCGCTCAATTTCCAAG-3'	**Sigma**

Table S7: Site-directed mutagenesis primers

Site	Primer Sequence	Source
K-H R106A Forward	5'-GAAGGCTGTAAAAAACCTTTAGAAGCATTGCTGAACATCTGGCAAGAAC-3'	**Sigma**
K-H R106A Reverse	5'-GTTCTTGCCAGATGTTCAGCAATGCTTCTAAAGGTTTTTTACAGCCTTC-3'	**Sigma**

Supplementary Methods

Western Blot Analyses. Protein concentrations were determined by BCA Assay following manufacturer's instructions (Thermo Scientific). Normalized protein samples were separated on denaturing gradient gels (4-20% from BioRad) and were transferred to PVDF membranes for immunoblotting. After transfer, the membranes were first blocked with 1X Sigma Blocking Buffer for an hour at room temperature. The membranes were then incubated with the indicated primary antibodies diluted in 1X Sigma Blocking Buffer at 4 °C overnight. After this step, the membranes were washed with PBST (3X, 10 minutes each). HRP-conjugated secondary antibodies were diluted in 1X Sigma Blocking Buffer and incubated with the membranes at room temperature for 1 h. After this incubation period, the membranes were washed with PBST (3X, 15 minutes each) and processed for chemiluminescence signal using the SuperSignal West Pico Substrate (Thermo Scientific) or Clarity Western ECL Substrate (BioRad).

Transfections. Briefly, cells were plated at log phase in 6- or 10-cm diameter wells in antibiotic-free medium the day before transfection. The following day, a mixture containing siRNA (e.g. in a 10 cm dish with final volume of 5 mL: 5 µL of 15 µM stock siRNA solution and Lipofectamine 2000 (10 µL) in Opti-MEM (1 mL total)) was prepared according to the manufacturer's instructions and added to cells with 4 mL of antibiotic-free medium dropwise, to give a final siRNA concentration of ~15 nM.

Proliferation Assays and EdU Click Chemistry. Asynchronous 231 shSCR versus shK-H cells were plated (40%) and grown in log-phase prior to treatment with EdU (10 μM) for 1 h at 37 °C in a humidified incubator (5% CO_2). After EdU treatment, the cells were trypsinized and gently washed with PBS (pH=7.4) prior to fixation with ice cold 70% ethanol at -20 °C overnight. After fixation, the cells were washed three times and rehydrated in 1% BSA/PBS at room temperature (5 min. intervals). The cells were then permeabilized with saponin/1%BSA/PBS solution for 1 h at 37 °C in a humidified incubator. After this step, the cells were washed with 1% BSA/PBS once, and incubated with the “”click” reaction mixture prepared as previously described [5, 6] but using Alexa-Fluor 647-azide as the conjugating azide dye (3 h). After incubation, the cells were washed twice with saponin/1%BSA/PBS (5 min. intervals). The cell pellets were then carefully dislodged in PI (10 μg/mL) diluted with saponin/1%BSA/PBS containing RNAse A (100 μg/mL) and incubated for 15 min at 37 °C in a humidified incubator prior to flow cytometer analysis. Flow cytometry experiments were immediately performed using the BD LSRFortessa II cell analyzer, and data were analyzed using the BD FACSDiva software (www.bdbiosciences.com).

PARP activity assays. Using silanized eppendorf tubes, reactions containing total protein lysates (90 μg in PBS) and excess blunt-ended DNA double-strand oligonucleotide (26-mer) with an internal synthetic abasic site in reaction buffer containing Tris-HCl (10 mM, pH=7.4) and Mg^{2+} (12 mM) were initiated by addition of excess β-NAD^+ (10 mM, freshly prepared). Reaction were stopped at various times (0-300 sec) by adding ice-cold AG014699/Rucaparib (250 μM), a known PARP1 inhibitor. Equal volume of reactants were analyzed on nitrocellulose membranes (BioRad dot blotter) and processed using standard Western blot assays with an antibody specific for PAR moieties (**Table S3**). Dot densities were quantified by NIH Image J and plotted using GraphPad PRISM after normalization to controls (no NAD^+ addition).

Immunofluorescence. shSCR or shK-H 231 cells were plated on six-well dishes (~200,000 cells/well) containing a glass slide overnight. Cells were then

treated with DMSO (0.01%) or Rucaparib/AG014699 (5 µM) for 24 h. Cells were washed and gently replaced with drug-free media and cells fixed at various times (0, 1, 6, 24 h) by gentle washing in phosphate-buffered solution (pH=7.4), followed by fixation with ice-cold methanol:acetone (3:1, v/v) for 10 min at -20 °C. Fixed and permeated cells on each slide were washed and rehydrated with PBS at room temperature (3X, 5 min intervals). Next, the cells were incubated in blocking solution (5% normal goat serum in PBS) for 60 min at RT. After blocking, the cells were then incubated in primary antibody (diluted in 5% normal goat serum in PBS) overnight at 4 °C. The next day, the cells were washed three times with wash buffer (1% BSA in PBS; 5 min. interval between washes). The cells were incubated in fluorescent secondary antibody diluted in 1%BSA/2.5% normal goat serum/PBS solution for 1 h at RT with minimal exposure to light. The cells were then washed three times with wash buffer (1% BSA in PBS; 5 min. intervals). Finally, the last wash buffer was completely aspirated, and the cover glass was mounted with Vectashield mounting medium with DAPI. Images were acquired using DM5500 Upright microscope (Leica) equipped with a digital camera. See **Table S3** for a list of specific antibodies and dilutions used.

Molecular Modeling. Homology modeling studies for K-H were prepared based on previously crystallized structure of RTT103 bound to pS2-CTD heptapeptide fragment of RNAPII CTD tail [7] to determine crucial K-H●RNAPII molecular interactions. Briefly, K-H and RTT103 primary sequences were aligned, and subjected for homology alignment using the coordinates of RTT103 to build K-H putative structure. These studies were performed prior to the recent release of K-H RPR domain crystal structure [8]. Molecular Operating Environment (MOE, www.chemcomp.com) and PyMol programs were utilized for modeling, simulation, and visualization of structures as previously described [9].

Luciferase Reporter Assays. Cells were plated into each well of a 6-well plate at log phase prior to transfection. For the knockdown experiments, siSCR or siK-H (15 nM) were first incubated in ~250 µL serum-free OPTI-MEM (TUBE A). In a

separate tube containing ~250 µL serum-free OPTI-MEM, RNAiMax (5 µL) was added (TUBE B). After brief incubation, the content of TUBE A was carefully mixed in with TUBE B and incubated at room temperature for 30 minutes. After this incubation, the solution was gently added dropwise into each well of cells in ~1 mL of media. The cells were then placed in the incubator for 24 h. After 24 h, the media was aspirated and replaced with a fresh media for a second round of transfection. This time, siSCR or siK-H (15 nM) were first mixed and incubated with pWTCDK1-Luc or a mutated derivative (1 µg) and Renilla Luciferase plasmid (5 ng) in ~250 µL serum-free OPTI-MEM (TUBE A). In a separate tube containing ~250 µL serum-free OPTI-MEM, Lipofectamine 2000 (5 µL) was added (TUBE B). After brief incubation, the contents of TUBE A was carefully mixed in with TUBE B and incubated at room temperature for 30 minutes. After this incubation, the solution was gently added dropwise into a well of cells in ~1 mL of media. The cells were then placed in the incubator for 48 hours. After incubation, cells were trypsinized, harvested and washed with PBS (2x). The pellets were then lysed in Passive Lysis Buffer (Promega) (100 µL). To assay firefly luciferase activity (expression driven by the CDK1 promoter), luminosity was measured after 20 µL of lysate was mixed with 100 µL of the Dual-Glo® Luciferase Assay Reagent in a 96-well plate. To measure *Renilla* luciferase activity, luminosity was measured again after addition of 100 µL of the Dual-Glo® Stop & Glo® Reagent. The activities of the experimental reporter (firefly luciferase) were normalized to the activities of the internal control reporter (*Renilla* luciferase). Reported promoter activities were relative to the siSCR and/or empty vector-treated control as indicated.

For transient protein overexpression experiments, cells ($1X10^6$) were plated into each well of a 6-well plate and allowed to reach log-phase growth in 24 h prior to transfection. Empty vector, K-H wild-type or mutant K-H_{R106A} cDNA expression plasmids (1 µg) were mixed with pWTCDK1-Luc containing wild-type, or mutated CDK1 promoter sequences (1 µg) and CMV-Renilla plasmid DNA (5 ng) in serum-free OPTI-MEM. To this, serum-free OPTI-MEM, Lipofectamine 2000 was added

and incubated at 30 mins at room temp. The solution was then gently added dropwise into separate wells and cells were then incubated 48 h.
After incubation, cells were trypsinized, harvested and washed twice with PBS. Cell pellets were then lysed in Passive Lysis Buffer (Promega) and firefly luciferase activity (luminosity, expression driven by the CDK1 promoter), monitored using Dual-Glo® Luciferase Assay Reagent in a 96-well plate. Simutaneously, *Renilla* activities were monitored using the Dual-Glo® Stop & Glo® Reagent. Firefly luciferase levels were normalized to the activities of the internal control reporter (*Renilla*). Each assay was assessed in triplicate in at least two different cell lines.

HR Activity Assays. Briefly, log-phase DR-GFP integrated cells[10] were transfected with siRNA (15 nM) against endogenous RAD51, CDK1, K-H or non-targeting scrambled control (SCR) using RNAiMax. After 24 h, cells were co-transfected with specific siRNAs indicated above, with or without myc-K-H or CDK1 cDNA expression plasmids (1 µg) and *I-SceI* plasmid (1 µg) using Lipofectamine 2000 as described [10]. GFP expression was quantified by flow cytometry after 72 h using a BD LSRFortessa II Cell Analyzer.

Co-immunoprecipitation (Co-IP) analyses. Log-phase cells were plated in 10-cm dishes, transfected with myc-tagged wild-type or mutant K-H^{R106A}, or empty pCMV-myc vector alone constructs for 48 h using Lipofectamine 2000. After transfection, cells were harvested and lysates (1 mg) were first pre-cleared with Protein A/G beads (Santa Cruz) prior to overnight incubation with 2 µg of anti-myc primary antibody or IgG control conjugated to Protein A/G beads at 4 °C. After incubation, beads were gently washed with TNEN solution [20 mM Tris–HCL (pH 8.0), 0.1 M NaCl, 1 mM EDTA, 0.05% NP-40] (3X, 5 min each using a rotator), then washed with PBS, and samples boiled in 2X protein loading buffer. Co-IPed proteins (e.g., RNAPII, B-MYB) were analyzed by Western blotting as described [11].

TUNEL Assays. To measure apoptotic cell death, log-phase shSCR or shK-H 231 cells were treated with vehicle (0.1% DMSO) or Rucaparib (5 or 10 μM) for 24 h, and incubated in drug-free media for an additional 72 h. Cells were then harvested, and fixed in 70% ethanol overnight at -20 °C. Cells (5 X 10^6) from each treatment were then subjected to terminal deoxynucleotidyltransferase dUTP nick-end labeling (TUNEL) using the APO-Direct TUNEL Assay kit (BD Biosciences), which includes positive and negative controls. Flow cytometry assays were performed in triplicate using a BD LSRFortessa II cell analyzer, and data were analyzed using BD FACSDiva software (www.bdbiosciences.com).

Supplementary References

1. Johnson, N. *et al.* Cdk1 participates in BRCA1-dependent S phase checkpoint control in response to DNA damage. *Molecular cell* **35**, 327-339 (2009).
2. Johnson, N. *et al.* Compromised CDK1 activity sensitizes BRCA-proficient cancers to PARP inhibition. *Nature medicine* **17**, 875-882 (2011).
3. Vichai, V. & Kirtikara, K. Sulforhodamine B colorimetric assay for cytotoxicity screening. *Nature protocols* **1**, 1112-1116 (2006).
4. Kao, J. *et al.* Molecular profiling of breast cancer cell lines defines relevant tumor models and provides a resource for cancer gene discovery. *PloS one* **4**, e6146 (2009).
5. Motea, E.A., Lee, I. & Berdis, A.J. A non-natural nucleoside with combined therapeutic and diagnostic activities against leukemia. *ACS Chemical Biology* **7**, 988-998 (2012).
6. Motea, E.A., Lee, I. & Berdis, A.J. Development of a 'clickable'non-natural nucleotide to visualize the replication of non-instructional DNA lesions. *Nucleic acids research* **40**, 2357-2367 (2012).
7. Lunde, B.M. *et al.* Cooperative interaction of transcription termination factors with the RNA polymerase II C-terminal domain. *Nature structural & molecular biology* **17**, 1195-1201 (2010).
8. Ni, Z. *et al.* RPRD1A and RPRD1B are human RNA polymerase II C-terminal domain scaffolds for Ser5 dephosphorylation. *Nature structural & molecular biology* **21**, 686-695 (2014).
9. Motea, E.A., Lee, I. & Berdis, A.J. Insights into the roles of desolvation and pi-electron interactions during DNA polymerization. *Chembiochem : a European journal of chemical biology* **14**, 489-498 (2013).
10. Bolderson, E. *et al.* Phosphorylation of Exo1 modulates homologous recombination repair of DNA double-strand breaks. *Nucleic Acids Res* **38**, 1821-1831 (2010).
11. Morales, J.C. *et al.* Kub5-Hera, the human Rtt103 homolog, plays dual functional roles in transcription termination and DNA repair. *Nucleic Acids Res* **42**, 4996-5006 (2014).